

Continuous synthesis of star polymers with RAFT polymerization in cascade microreactor systems

Liang Xiang^a, Min Qiu^a, Minjing Shang^a, Yuanhai Su^{a,b,*}

^a School of Chemistry and Chemical Engineering, Frontiers Science Center for Transformative Molecules, Shanghai Jiao Tong University, Shanghai, 200240, PR China

^b Key Laboratory of Thin Film and Microfabrication (Ministry of Education), Shanghai Jiao Tong University, Shanghai, 200240, PR China

ARTICLE INFO

Keywords:

Microreactor
RAFT polymerization
Star polymer
Emulsification

ABSTRACT

With the RAFT arm-first method, butyl acrylate and 4-acryloylmorpholine were used as monomers to form linear arms, which subsequently reacted with the cross-linker 1,6-hexanediol diacrylate to form star-shaped macromolecules in cascade microreactor systems. After studying polymerization kinetics in each step, homoarm and miktoarm star products with various arm compositions were steadily prepared by optimizing the reaction flowsheet and adjusting the reactant formula. Such continuous-flow processing avoided tedious intermediate purification procedures and prepared polymer products with considerable star yield (>70%), molecular weights ($M_{w,LS} > 100$ kg/mol) and arm numbers (>30). Multiple emulsions (including two types, i.e., oil-in-water and water-in-oil) were formed utilizing star products with different amphiphilic architectures as emulsifiers. This study demonstrated that in this continuous-flow mode, through regulating the residence time and flow rate ratio in each step, the arm and core structures of star polymers were tailored to possess remarkable functional applications.

1. Introduction

Star polymers, which contain at least three linear chains radiating from a central core, are one special class of branched polymers. Owing to their spatially defined (i.e., core-shell-periphery) yet highly compact three-dimensional structure configuration, star polymers possess significantly different physicochemical properties (e.g., rheological and thermal properties) compared to their linear counterparts [1,2]. Based on chemical compositions of arms, star polymers can be classified into two subsets, including homoarm star polymers and miktoarm star polymers. The former ones consist of symmetrical arms with identical chemical compositions and molecular weights, while the latter possess chemical asymmetry (chemically different arms) or molecular weight asymmetry (unequal arms) [2]. Different properties of arms and the core enable star polymers to have microphase separations in bulk, solution, and other interfaces [3]. The segregated compartments in the formed aggregates, such as micelles, can provide distinct chemical environments to store various kinds of small molecules [4,5]. Hence, star polymers have broad applications in catalysis, emulsification, photonics, drug delivery and so on [1,6].

While different techniques such as anionic/cationic polymerization

[7,8] and ring-opening polymerization [9] have been employed to prepare star polymers, the rise of reversible deactivation radical polymerization (RDRP) techniques [2,6], including nitroxide-mediated polymerization (NMP), atom transfer radical polymerization (ATRP), and reversible addition-fragmentation chain transfer radical polymerization (RAFT), paves the way for synthesizing star polymers from a large range of monomer families without requiring stringent reaction conditions. Using RDRP techniques, star polymers are usually prepared via the so-called core-first, arm-first and grafting onto approaches, based on the sequence of the formation of the core and the arms. The core-first approach [10,11] starts from a multifunctional initiator (i.e., the core) so that the number of arms of the product is precisely determined. In the arm-first approach [12,13], linear chains are prepared and serve as arm precursors, and then the arms are binding to the core via copolymerization with cross-linkers. In this way, the number of arms is undefined, yet high control over the arm length is achieved. Notably, this approach is ideal for the synthesis of miktoarm star polymers. In the grafting onto approach [14], linear arm precursors are attached to a multifunctional core to create a star polymer, usually via specific coupling reactions such as click chemistry.

Microreactor technology is recognized as a promising process

* Corresponding author. School of Chemistry and Chemical Engineering, Frontiers Science Center for Transformative Molecules, Shanghai Jiao Tong University, Shanghai, 200240, PR China.

E-mail address: y.su@sjtu.edu.cn (Y. Su).

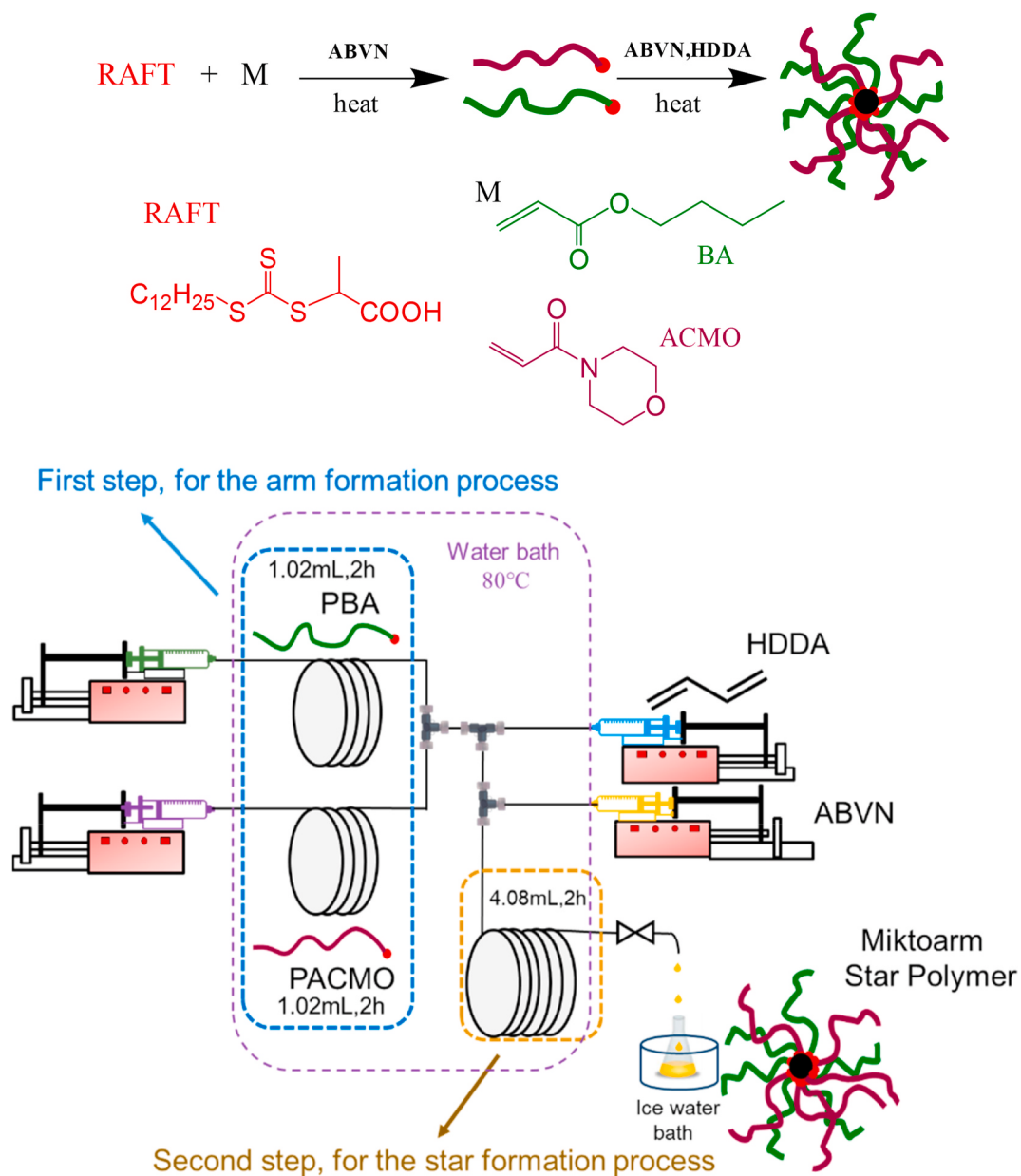


Fig. 1. Schematic overview of the cascade microreactor system for the synthesis of PACMO-PBA miktoarm star polymer sample MSPA₅₀.

intensification technology for a broad range of reaction processes in laboratory and industry. The features of microreactors such as larger surface-to-volume ratio, higher mixing efficiency, faster heat and mass transfer rates, and excellent spatiotemporal control, allow reaction processes to overcome the transport limitation and thus to have better performance (e.g., higher selectivity and yield) compared with conventional batch reactors. The entire operation processes in microreactors are streamlined from start to end, which improves production efficiency and reduces manufacturing cost. Moreover, by extending the microchannel length or simply operating multiple microchannels in parallel, microreactor systems can be readily scaled up to meet industrial production [15,16]. Up to date, microreactors have been reported to have plenty of applications in polymer chemistry [17]. Combined with the RDRP technology of strong molecular design capability, tailor-made polymers with various sequence compositions, such as gradient [18], multiblock [19] and unimolecular sequence-defined [20], have been synthesized in microreactors, displaying enhanced precision than those from batch counterparts [21–23].

Concerning the topology structure of polymers, continuous synthesis of complex architectures such as hyperbranched [24,25], cyclic [26], star [27], and brush polymers [28] has been gradually realized with the use of microreactors in recent years. In particular, the synthesis of star polymers is rather complicated since monomers and cross-linkers should be polymerized sequentially with either the core-first or arm-first approach [29]. Considering that star polymers have wide industrial applications and its preparation typically requires the synergistic design on both the reactor construction and the operation procedure, the exploration of the continuous process with potential scale production capabilities will be a rational yet challenging avenue.

Hitherto, there are only a few reports on the continuous synthesis of star polymers. In 2016, Junkers' group reported the continuous synthesis of star polymers utilizing the microreactors for the first time [27]. Following the core-first approach, star polymers with 4–21 arms were synthesized via photo-initiated copper-mediated polymerization in a UV-microflow reactor. The arm chains were further extended towards multiblock copolymer structures, and thereby the hierarchically

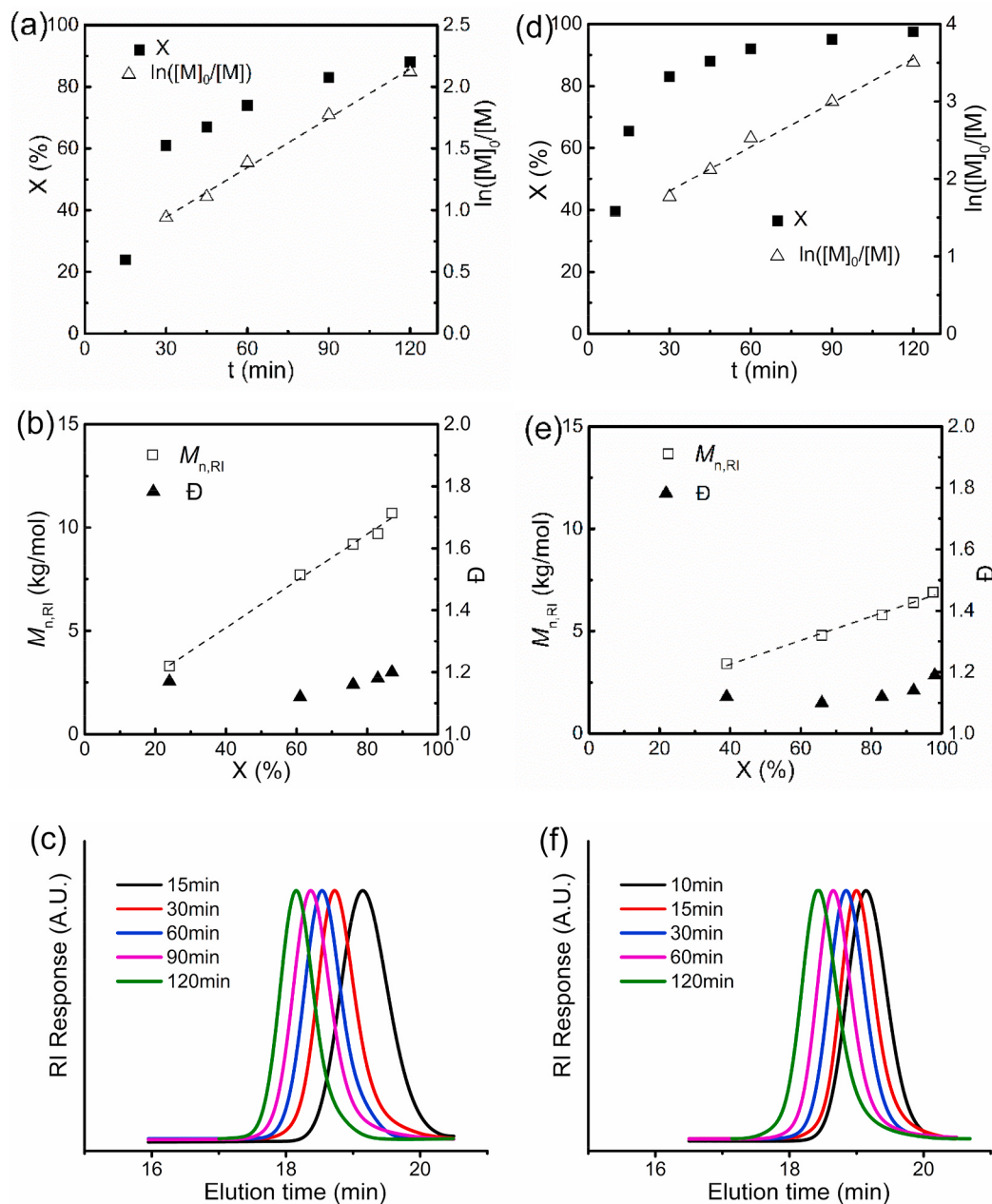


Fig. 2. a,d) $\ln([M]_0/[M])$ and the monomer conversion (X) vs the residence time (t), b,e) the number-average molecular weight ($M_{n,RI}$) and polydispersity (D) vs X , and c,f) GPC traces (RI) of linear (a)-(c) PBA and (d)-(f) PACMO samples collected from the microreactor system (Polymerization condition: $[M]_0/[DoPAT]_0/[ABVN]_0 = 100/1/0.1$, $[M]_0 = 2.5$ M).

structured product could show pH responsiveness and self-assembly in the aqueous phase. Moreover, Junkers et al. explored the continuous preparation of star polymers using the arm-first approach, and a cascade microreactor was built to combine arm and star synthesis processes, producing miktoarm and surface functionalized star polymers [30].

Inspired by Junkers' research, we developed a homemade cascade microreactor system to synthesis star polymers utilizing the RAFT arm-first method. In this work, polymerization kinetics in the arm and star formation steps were studied, and the effects of reaction time, mixing performance and reactant formula on final product structures (e.g., star yields, molecular weights and arm numbers) were thoroughly investigated in order to achieve optimized molecular design. Moreover, by adjusting residence times and the flow rate ratio of the different streams, various arm compositions were targeted. Star products were conveniently prepared in this continuous-flow processing, which had lower

critical micelle concentration (CMC) values than small-molecule emulsifiers and could be directly applied to form various types of emulsions.

2. Experimental

2.1. Materials and apparatus

Butyl acrylate (BA, Sinopharm) was purified by washing with sodium hydroxide aqueous solution and deionized water, then was dried with 4A molecular sieves. 4-Acryloylmorpholine (ACMO, Aladdin) was purified through a basic alumina column to remove the inhibitor. 2, 2'-Azobis(dimethylvaleronitrile) (ABVN, 98 wt %, Energy Chemical), 1,6-hexanediol diacrylate (HDDA, 90 wt %, Aladdin), 1,3,5-trioxane (Aladdin), N,N-dimethylformamide (DMF, Sinopharm), tetrahydrofuran (THF, Sinopharm) and methylene blue (Aladdin) were all used

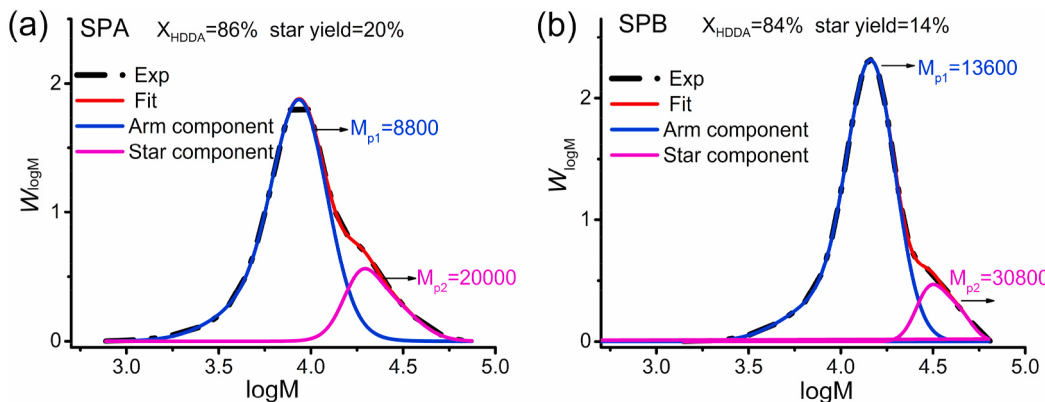


Fig. 3. Deconvolution of the MWDs for the homoarm star polymers collected from the cascade microreactor system (Polymerization condition: $[M]_0/[RAFT]_0/[ABVN]_0 = 100/1/0.1$ in the first step, $[CL]_0/[RAFT]_0/[ABVN]_0 = 10/1/0.2$ in the second step, and $[M]_0 = 2.5\text{ M}$).

without further purification. The RAFT agent, 2-(dodecylthiocarbonothioylthio) propionic acid (DoPAT), was synthesized according to the literature procedure [31].

Poly ether ketone (PEEK) T-micromixers, unions, and perfluoroalkoxy (PFA) capillaries were purchased from IDEX Health & Science Inc. (United States). The capillaries applied were all of the 1/16 inch O.D. and 1.00 mm I.D., with the length being chosen for the given application. The high-pressure syringe pumps were purchased from New Era Pump Systems Inc. (United States).

2.2. Synthesis

2.2.1. Synthesis of linear polymers in the microreactor

Typically, for the synthesis of linear PBA, a homogeneous solution was obtained by adding the monomer BA (2.5 M, 100 eq), the RAFT agent DoPAT(1 eq), the initiator ABVN (0.1 eq) and the solvent DMF into a dried flask sealed with a rubber septum, and then was purged with N_2 for 30 min. A capillary microreactor with 1.02 mL inner volume was flushed with dry DMF to purge moisture and oxygen inside the system. Then the reaction mixture was introduced into the microreactor by a syringe pump at the designed flow rate. The microreactor was immersed in a water bath at 80 °C.

After the flow inside the capillary microreactor reached a stable state, the effluent was collected by a vial immersed in an ice-water bath. Following solvent removal and re-dissolving in dichloromethane, the polymer product was precipitated in cold ethanol, filtrated and dried under vacuum at 70 °C for 12 h. Other linear polymers, e.g., homopolymers PACMO and random copolymers P(ACMO-ran-BA), were synthesized in the same way by varying the ACMO/BA molar ratio while keeping the total monomer concentration constant at 2.5 M.

2.2.2. Synthesis of homoarm star polymers in the cascade microreactor system

Typically, for the synthesis of PBA homoarm star polymer (SPB) with the molar ratio of $[BA]_0/[DoPAT]_0/[HDDA]_0 = 100/1/10$, the mixture of BA (2.5 M, 100 eq), DoPAT (0.025 M, 1eq), ABVN (2.5 mM, 0.1eq) and DMF were used to prepare linear arms. HDDA (0.5 M) dissolved in DMF and ABVN (0.01 M) dissolved in DMF were ready for the cross-linking process. After the oxygen removal, they were loaded into separate gastight syringes. Two syringes containing the reaction solutions with the same compositions for the arm formation step were connected to two separate capillary microreactors with the same inner volume of 1.02 mL (Fig. S2a), with a targeted residence time τ_1 of 2 h at a flow rate of 0.51 mL/h. Indeed, one syringe should be sufficient for this step. However, we adopted this kind of “pseudo-miktoarm” operation to stay close to the subsequent synthesis processes for miktoarm star polymers [30]. Afterwards, the cross-linker mixture and initiator mixture

feedstocks (both at the flow rate of 0.51 mL/h) mixed with the stream of synthesized linear polymers through two micromixers, so the concentrations of reactants were diluted according to their flow rate ratio (Fig. S1). The newly combined stream was delivered into a second capillary microreactor with 4.08 mL for the star formation step, at a residence time τ_2 of 2 h (total flow rate of 2.04 mL/h). Samples at steady state were collected after twice the total residence time τ ($\tau = \tau_1 + \tau_2$). Other homoarm star polymers with homopolymer or copolymer arms were synthesized similarly but by varying the ACMO/BA ratio at the first step for arm formation (Fig. S2b).

2.2.3. Synthesis of miktoarm star polymers in the cascade microreactor system

Fig. 1 presents a schematic diagram of the experimental setup for the synthesis of PACMO-PBA miktoarm star polymers (sample MSPA₅₀). The entire synthesis process used a similar procedure to that for homoarm star polymer, except that the corresponding two syringes contained different monomers (ACMO and BA) at the first step. The experimental setup was fine-tuned to prepare other miktoarm star polymers, i.e., samples MSPA₂₅ and MSPA₇₅ (see Fig. S3). Miktoarm star polymers with different arm compositions were tailored by regulating the flow rate ratio of the two streams in the arm formation step. To maintain the same residence time τ_1 (2 h) of the two streams producing different arm species in this step, their total flow rate was maintained constant and the volumes of two parallel capillaries were adjusted proportionally (Table S1).

3. Results and discussion

3.1. RAFT polymerization for linear arms in the microreactor

We first investigated the continuous-flow preparation of linear arms. BA and ACMO were selected as target monomers because their corresponding polymer chains were respectively hydrophobic and hydrophilic, which could be used to fabricate miktoarm star polymers. The highly active initiator ABVN was selected to ensure fast reaction rates as to avoid long reaction time. By adjusting the feed flow rate to achieve different residence times, we studied the RAFT homopolymerization kinetics of BA and ACMO, as shown in Fig. 2. Upon entering the capillary microreactor, the reaction mixture was heated from the room temperature to the set temperature and established the RAFT equilibrium. Although such a process was greatly benefited from the enhanced heat and mass transfer in the microreactor, the influence of this inhibition period on the conversion (X) could not be ignored especially when the residence time was short [32,33]. Only after the residence time exceeded 30 min, the polymerization processes fitted the first-order kinetics well (Fig. 2a, d), indicating that the amount of active radicals remained

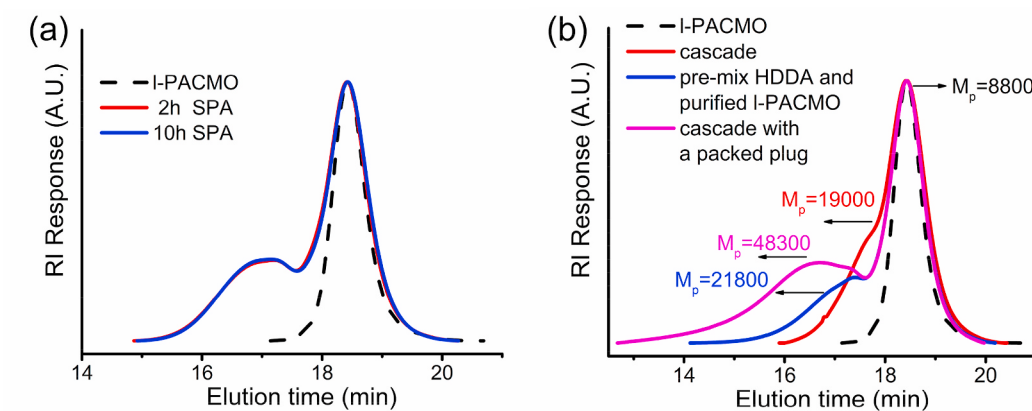


Fig. 4. GPC traces (RI) of PACMO homoarm star polymers (SPA) (a) collected at different reaction times, $[CL]_0/[arm]_0/[ABVN]_0 = 10/1/0.2$; (b) collected from the microreactor with different mixing performance.

Table 1

Summary of homoarm star products prepared in the cascade microreactor system.

Entry ^a	$[M]_0$ (M)	Arm formation				Star formation				Star yield ^e (%)
		$[M]_0/[RAFT]_0$	X_M ^b (%)	$M_{n,a}$ ^c (kg/mol)	D_a ^d	$[CL]_0/[RAFT]_0$	X_{CL} ^b (%)	$M_{w,s}$ ^d (kg/mol)	D_s ^d	
1 ^f	2.5	100	98	6.9	1.19	10	86	23.6	1.14	20
2 ^f	2.5	40	99	3.2	1.17	10	92	63.6	2.13	75
3 ^f	1.25	20	98	1.8	1.16	10	91	36.1	2.17	92
4 ^g	\	0	\	\	\	10	88	77.1	2.60	\
5 ^f	2.5	40	99	3.2	1.17	5	89	14.6	1.36	51
6 ^{f,i}						15				
7 ^f	1.25	40	98	3.1	1.19	10	78	19.5	1.50	56
8 ^f						15	81	41.8	2.41	70
9 ^{f,i}						20				
10 ^h	2.5	100	87	10.8	1.20	10	84	35.2	1.13	14
11 ^h	2.5	40	90	4.6	1.20	10	90	90.6	2.38	72

^a Polymerization conditions: $T = 80^\circ\text{C}$; The residence times for both the arm formation and star formation steps were 2 h.

^b X_M and X_{CL} were conversions of the monomer, cross-linker, respectively.

^c $M_{n,a}$, D_a were apparent number-average molecular weight and polydispersity of linear arms, measured by the RI detector.

^d $M_{w,s}$, D_s were apparent weight-average molecular weight and polydispersity of star components, calculated from the peak analysis of the MWD curves (RI) of the star products.

^e Determined by the multi-peak splitting of the MWD curves (RI).

^f ACMO was the monomer for the arm formation.

^g Branched PHDDA was prepared from the homopolymerization of HDDA (0.3125 M) mediated by DoPAT.

^h BA was the monomer for the arm formation.

ⁱ The channel blockage occurred.

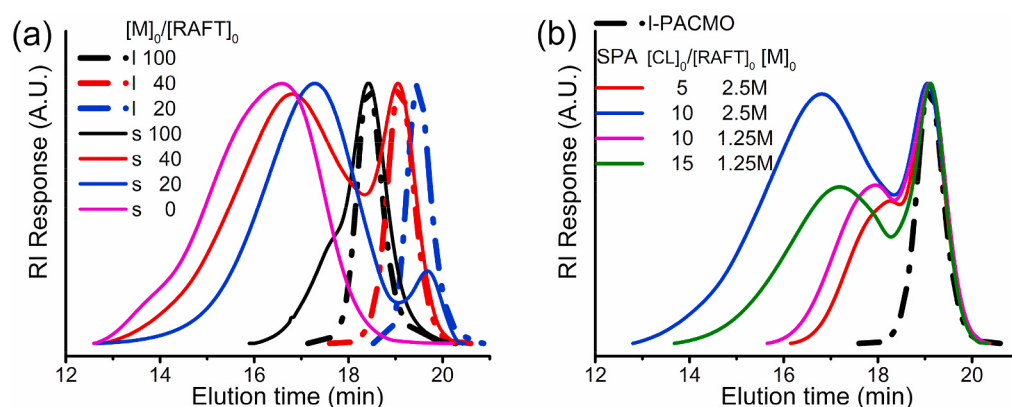


Fig. 5. GPC traces (RI) of I-PACMO and SPA (a) with different arm lengths ($[M]_0/[RAFT]_0 = 100, 40, 20$; $[CL]_0/[RAFT]_0 = 10$); (b) with different amounts of cross-linker ($[M]_0/[RAFT]_0 = 40$; $[CL]_0/[RAFT]_0 = 5, 10, 15$; $[M]_0 = 2.5, 1.25$ M).

constant. The linear increase of the number-average molecular weight ($M_{n,RI}$) with X as well as the narrowly distributed GPC traces ($D < 1.2$) confirmed that both the polymerization processes of BA and ACMO

displayed living features mediated by DoPAT.

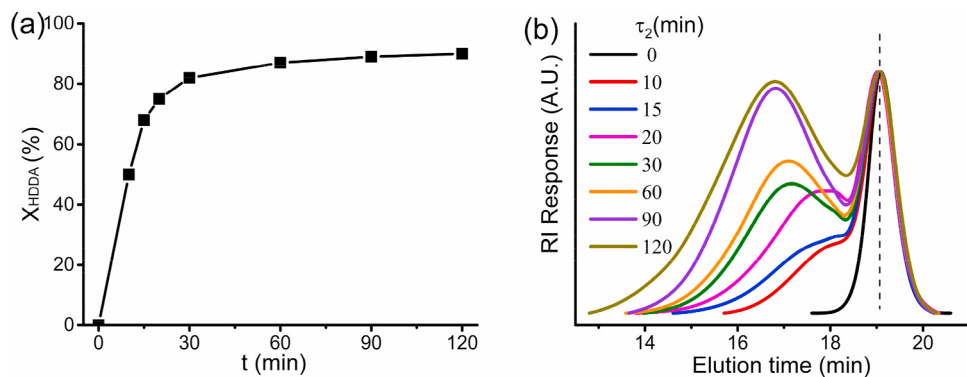


Fig. 6. (a) HDDA conversion vs τ_2 ; (b) GPC traces (RI) of SPA at different τ_2 .

Table 2

Summary of the star products with various arm compositions prepared in the cascade microreactor system.

Sample ^a	Arm formation						Star formation					n_1/n_2^g	N_{arm}^h
	X_{ACMO} ^b (%)	X_{BA} ^b (%)	$M_{w,a}^c$ (kg/mol)	D_a^c	α_a^d	$R_{h,w}^e$ (nm)	X_{CL} ^b (%)	$M_{w,s}^c$ (kg/mol)	Star yield ^f (%)	α_s^d	$R_{h,w}^e$ (nm)		
SPA	99	\	5.0	1.02	1.26	2.04	92	266.0	75	0.51	6.23	\	38
SPB	\	90	6.1	1.09	0.70	2.14	90	387.3	72	0.28	8.70	\	35
SPA ₂₅ ^j	94	90	5.4	1.09	0.75	2.12	86	362.2	70	0.32	8.29	26/74	40
SPA ₅₀ ^j	95	91	5.5	1.08	0.87	2.19	88	299.6	76	0.35	8.85	51/49	36
SPA ₇₅ ^j	96	94	5.7	1.04	0.78	2.11	89	258.1	73	0.42	6.39	75/25	31
MSPA ₂₅ ^j	99	90	Two kinds of homopolymer arms				88	325.8	73	0.33	8.88	28/72	35
MSPA ₅₀ ^j							89	258.6	78	0.31	7.23	56/44	31
MSPA ₇₅ ^j							90	224.9	76	0.39	6.50	79/21	29

^a Polymerization conditions: T = 80 °C; in the first step, [M]₀/[RAFT]₀/[ABVN]₀ = 40/1/0.1, [M]₀ = 2.5 M, τ_1 = 2 h; in the second step, [RAFT]₀/[CL]₀/[ABVN] = 1/10/0.2, [CL]₀ = 0.3125 M, τ_2 = 2 h.

^b X_{ACMO} , X_{BA} and X_{CL} were conversions of ACMO, BA and HDDA, respectively.

^c Absolute weight-average molecular weight $M_{w,a,LS}$ and $M_{w,s,LS}$ of star polymers, as well as polydispersity $D_{a,LS}$ of arms, measured by the LS detector.

^d α_a and α_s were the Mark-Houwink exponent values of arms and star products respectively, measured by the DP detector.

^e Weight-average hydrodynamic radius ($R_{h,w}$) of the arms and star products, measured by the DP detector.

^f Star yields, determined from the peak analysis of the MWD curves (RI).

^g Molar ratio of ACMO to BA units or the arm composition ratio of l-PACMO to l-PBA in star products.

^h N_{arm} , calculated as seen in the Supporting Information.

ⁱ SPA_i, i represented the initial mole percentage of ACMO units for copolymer arms in homoarm star products.

^j MSPA_i, i represented the designed mole percentage of l-PACMO arms in miktoarm star products.

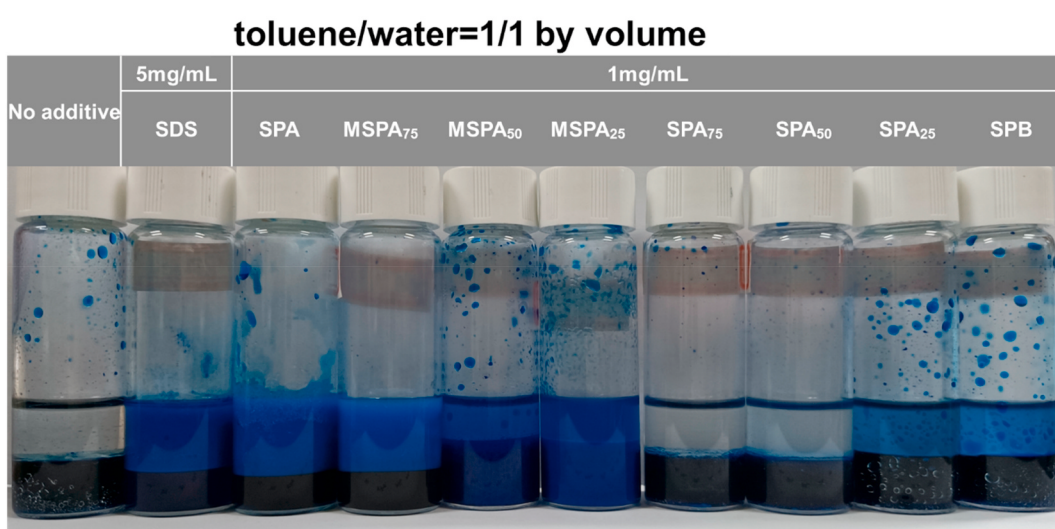


Fig. 7. Photographs of toluene/water emulsion samples stabilized by different star products after preparation for 7 days.

Table 3

Phase occupation for emulsion systems prepared using increasing volumetric fractions of toluene solutions of star products (1 mg/mL).

Sample ^a	15% ^b			30% ^b			50% ^b			60% ^b			70% ^b		
	O.	E.	W.												
MSPA₂₅	19%	8%	73%	20%	30%	50%	33%	67%	0	51%	49%	0	62%	38%	0
%															
MSPA₅₀	0	28%	72%	0	44%	56%	38%	62%	0	55%	45%	0	64%	36%	0
MSPA₇₅	0	33%	67%	0	51%	49%	0	68%	32%	0	81%	19%	0	91%	9%
SPA^c	0	34%	66%	0	47%	53%	0	62%	38%	5%	78%	17%	10%	80%	10%

^a The volume percentage of oil(O.) emulsion(E.) and water phase (W.) in the emulsion samples was measured 7 days after preparation.

^b Volumetric fraction of toluene solution of star products when preparing the emulsion samples.

Table 4

Toluene/water interfacial tensions (mN/m) for star product solutions.

Additive	Pure toluene/ water	SDS	MSPA ₂₅	MSPA ₅₀	MSPA ₇₅	SPA
1 mg/ mL	25.95 ± 0.71	3.37 ± 0.14	3.46 ± 0.17	1.36 ± 0.38	10.74 ± 0.38	13.42 ± 0.25

3.2. Study on the reaction conditions for preparing star polymers in the cascade microreactor system

During the aforementioned process for preparing arms, the conversion of ACMO reached 98% in 2 h, which was higher than that of BA (87%). In similar systems, the monomer conversion between 80 and 90% should be sufficient for the continuous preparation of block polymers [34]. Therefore, the residence time for the first step τ_1 was set at 2 h in our current work.

Both the arms, i.e., linear PACMO (l-PACMO) and linear PBA (l-PBA) synthesized in the first step bore a $-SC(Z)=S$ moiety at the chain end originating from the RAFT agent. The cross-linkers were copolymerized with arms through the chain extension, resulting in the formation of cross-linked cores in the second step. Therefore, the molar ratio of the cross-linker molecules to the arm chains theoretically corresponded to $[CL]_0/[RAFT]_0$. We tried to set the residence time of the second step τ_2 at 2 h and investigated the PACMO and PBA homoarm star polymer (SPA and SPB) formation processes at a $[CL]_0/[RAFT]_0$ of 10:1. However, as shown in Fig. 3, there appeared to be two major portions in molecular weight distribution (MWD) curves of the final products. The peak at the large MW portion was related to the star polymers, whereas the smaller MW portion was attributed to the residual (unreacted) arm precursors. Through a deconvolution technique to subtract the portion of the arm precursor component (assuming a Gaussian distribution) from MWD curves [35], it can be found that star yields of the collected samples were

all below 20%. Besides, the peak molecular weight of the star polymer component M_{p2} was only about twice larger than that of the arm component M_{p1} , indicating that the star polymer contained just a few arms. Such unsatisfactory results inspired us to analyze the parameters affecting the star formation process, as to determine the optimal reaction conditions for preparing star polymers with reasonable arm numbers and yields.

3.2.1. Effect of the reaction time of the second step

Assuming the arm precursors might not fully undergo the coupling reaction with cross-linkers at τ_2 of 2 h, we significantly prolonged the reaction time for this step (this experiment was conducted in the flask as a batch reactor, see details in Supporting Information). After taking product samples at the reaction times of 2 h and 10 h, it was surprising that the GPC traces for these two different reaction times almost overlapped (Fig. 4a). This was probably because the half-life period of the initiator ABVN was short at 80 °C (0.27 h in toluene), and the residual initiator content after 2 h was lower than 6% of the initial concentration. That is, the concentration of free radicals available for the chain initiation was low, restricting the followed chain transfer from long chains to short chains. Moreover, the mobility of the reactant segments was deficient, and thus the effect of the reaction time prolongation on the arm conversion was extremely limited.

3.2.2. Effect of the mixing performance

The mixing process between polymer segments with fresh monomers was reported to remarkably influence the MWDs in chain extension reactions [36,37]. Laminar flow profiles with low Reynolds numbers were obtained in our system, and the mixing process of different streams was dominated by the molecular diffusion [38], which could be enhanced by pre-mixing or utilizing auxiliary mixing equipment. For the second step, to eliminate the possible influence of uneven mixing, we first prepared a homogeneous mixture containing purified l-PACMO and HDDA, and then injected it into a capillary microreactor with 4.08 mL inner volume for the synthesis of SPA (more details in Supporting Information).

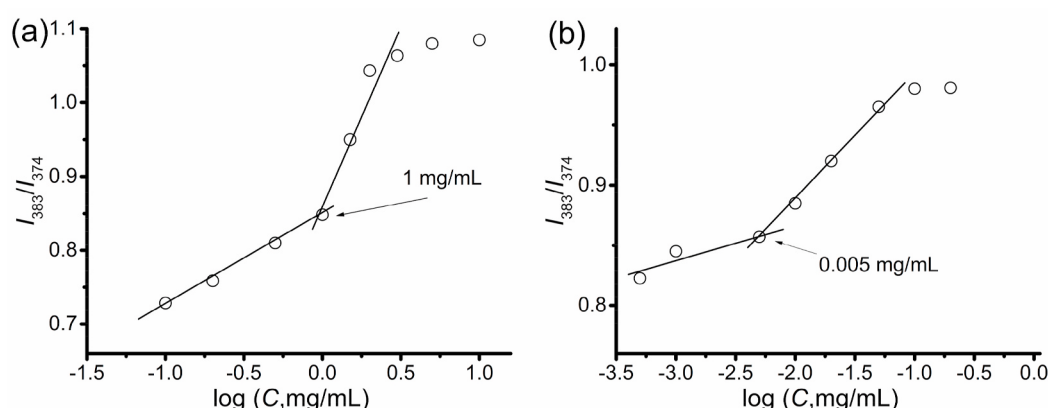


Fig. 8. CMC curves of (a) SDS and (b) SPA at different concentrations determined by the emission fluorescence spectra.

Accordingly, the GPC trace of the product moved slightly to a high MW region. Similar to Gao's report for preparing star polymers [39], the procedure of linear chains purification was omitted in our cascade microreactor system. Strictly speaking, the core was a copolymer of the cross-linker and the unreacted monomer. Such a structure could decrease the core's steric congestion, hence facilitating the incorporation of arms into the star polymer, and vice versa. Nevertheless, for the microreactor operation herein, unreacted monomers and initiators were removed from linear chains and the cores were formed merely by the cross-linkers, which might weaken the optimization effect of enhanced mixing on MWDs. Moreover, we hoped to avoid tedious intermediate procedures of purification, separation and solution preparation, so as to achieve the continuous preparation of the targeted polymers from reactants in the true sense.

Chen et al. proposed the use of a packed plug in flow RAFT systems, which improved the mixing between different streams and benefit the MWD control of block copolymers [36]. We adopted their idea, and thus a plug packed with 40 mesh size SiO_2 beads was assembled behind the T-micromixers for the second step in the cascade microreactor system (see Fig. S4). To our delight, more linear arms joined in the star structure, causing an obvious shift of the MWD curve to the high MW region. The peak molecular weight of the star polymer component M_{p2} was 5 times larger than that of the arm component M_{p1} (Fig. 4b), suggesting that the enhanced mixing performance was indeed beneficial for increasing the star yield. Unfortunately, in the later exploratory experiments using formulas with larger contents of cross-linkers, microgels could form and then be adsorbed by SiO_2 beads during the coupling reaction process. As the microgels aggregated, the resistance of the packed plug significantly increased and eventually blocked the microreactor system. It was difficult to rinse out the microgels from the packed plug effectively, and replacing the packed plug might affect the experiment's repeatability. Nevertheless, commercial mixing devices such as static micromixers [40] could be considered to replace packed plugs for further studies of mixing-related polymerization systems.

3.2.3. Effect of the reactant formula

We analyzed parameters such as arm chain length, monomer concentration and cross-linker/RAFT ratio in the reactant formula, as they have been reported to influence the properties of star polymers in batch operations [12,13]. Table 1 lists detailed information on the synthesis and characterization results of homoarm star samples prepared in the cascade microreactor system.

The arm chain length was controlled by the initial molar ratio of monomers to RAFT agents and the monomer conversions. In particular, ACMO was almost entirely consumed in 2 h and the corresponding arm chain length approximately equaled $[M]_0/[\text{RAFT}]_0$. When $[\text{CL}]_0/[\text{RAFT}]_0$ was maintained at 10, for samples from Entries 1–3, it could be seen from Fig. 5a that GPC traces of the products all exhibited bimodal distributions, inside which the low MW (high elution time) peak clearly overlapped with the linear arm peak. There were only a few examples reported without linear chains remaining for similar polymerization systems [12,30], and hence the observed behavior was rather typical. However, as the chain length of l-PACMO decreased from 100 to 20, the star yield for the corresponding product increased from 20% to 92%. Especially, for the sample from Entry 4, the product branched PHDDA could be regarded as a star polymer with the arm length of 0, and the GPC trace exhibited a unimodal distribution peak at a high MW region. At the star formation step, longer arms not only had weaker mobility but also occupied larger space, which hindered adjacent arms from accessing the core sites and contacting the cross-linkers. In this case, the coupling efficiency was reduced and fewer arms per a star polymer would be obtained. The homoarm star PBA (SPB) products from Entries 10 and 11 also revealed similar regularity.

On the other hand, the steric effect from longer arms limited the star-star coupling reaction, narrowing the MWD of the star polymer. For shorter arms, they were more effectively inserted into the star structure

and contributed more to the total molecular weight of the star polymer. Although the arm chain length was uniform, the star polymer was actually a mixture of star-shaped macromolecules with different arm numbers, and this heterogeneity could lead to D_s above 2.0. As confirmed by the samples from Entries 3 and 7, the shorter the arm length was, the higher $M_{w,s}$ and D_s were for the star components. Samples from entry 2 and 3 seemed to deviate from this trend because the effect of the monomer concentration must also be considered as discussed below.

Lower monomer concentration along with lower initiator and cross-linker content slowed down the polymerization rate while maintaining the values of $[M]_0/[\text{RAFT}]_0$ and $[\text{CL}]_0/[\text{RAFT}]_0$. Therefore, the HDDA conversion in Entry 7 was 78%, lower than that in Entry 2 (92%). Besides, there was less opportunity for the contact between polymer segments in the dilute system, thereby weakening star formation in Entry 7. Gao et al. [11] reported that intramolecular cyclization reactions were enhanced under dilute conditions, which consumed so many pendant vinyl groups of cross-linker units, being unconducive to the star yield.

The influence of the cross-linker dosage should not be ignored. During the synthesis of star polymers via the arm-first method, divinyl cross-linkers functioned to bind linear chains with the central core to form star-shaped macromolecules, and thus its content significantly affected the molecular weight and yield of star polymer. As seen in Fig. 5b, in the case of $[M]_0 = 2.5 \text{ M}$ and $[M]_0/[\text{RAFT}]_0 = 40$, the star yield was 51% when $[\text{CL}]_0/[\text{RAFT}]_0 = 5$. While increasing $[\text{CL}]_0/[\text{RAFT}]_0$ to 10, the star yield rose to 75%, as a larger amount of HDDA available enabled more arms to be incorporated into the star polymer, hence resulting in higher molecular weight and broader MWD. However, further increasing the HDDA content to a high value (i.e., $[\text{CL}]_0/[\text{RAFT}]_0 = 15$) brought the gelation risk, and the microreactor system was blocked up before we could collect a stable sample. In a more dilute system with $[M]_0 = 1.25 \text{ M}$, the gel point could be delayed, and the channel blockage occurred at $[\text{CL}]_0/[\text{RAFT}]_0 = 20$.

After analyzing parameters including the reaction time, mixing performance and reactant formula, we can conclude that the arm chain length and the HDDA dosage had remarkable effects on the star formation process. At $[M]_0/[\text{RAFT}]_0 = 40$, $[\text{CL}]_0/[\text{RAFT}]_0 = 10$, SPA and SPB with acceptable star yields (>70%) and molecular weights could be smoothly prepared in the cascade microreactor system.

3.2.4. Kinetics of the coupling reaction in the cascade microreactor system

Moreover, in the second step of the cascade microreactor system, we used l-PACMO with the chain length of nearly 40 as an example to study the coupling reaction kinetics from linear macromolecules to star-shaped macromolecules. The flow rate of the combined stream was maintained constant, and τ_2 was controlled by adjusting the inner volume of the capillary (V_2). Fig. 6 shows that the conversion of HDDA quickly exceeded 80% after 30 min. However, the reaction rate of HDDA decreased significantly when τ_2 was longer than 30 min, not only because of the falling HDDA concentration but also due to the majority of the radicals' encapsulation within the cross-linked cores, leading to the enhanced diffusion resistance for HDDA to travel through the PACMO shell to react with those radicals [41].

With the increase of the coupling degree, the star yield increased from 36% at $\tau_2 = 10 \text{ min}$ to a plateau value of 75% at $\tau_2 = 2 \text{ h}$. The MWD curve gradually expanded to the high MW region, but the trend would become less obvious. Therefore, τ_2 was selected as 2 h for the subsequent continuous synthesis of various star polymers.

3.3. Synthesis of star polymers with varied compositions in the cascade microreactor system

To demonstrate the versatility of our cascade microreactor system, we sought to expand experiments to synthesize star polymer products with various arm compositions. For homoarm star polymers, the arms could be homopolymers (l-PACMO or l-PBA) or random copolymers l-P

(ACMO-ran-BA). For miktoarm star polymers, the arms were compromised of two kinds of linear chains (l-PACMO and l-PBA), and their molar ratios were tuned by adjusting the flow rate ratio of the two streams containing different monomers in the arm formation step. Table 2 lists the polymerization results of these star polymers, in which the molecular weight data from the LS detector were used to calculate the arm numbers. All kinds of linear arms were well synthesized with D_a , _{LS} less than 1.10. The Mark-Houwink exponent values of the star products α_s were lower than those of the corresponding arms α_a , suggesting that densely packed three-dimensional structures were formed after the star formation process [24]. In THF, the hydrodynamic radius of the star products was 6–9 nm, which was larger than ~2 nm of the linear arms and was consistent with the conformation characteristics of the star-shaped polymer reported in literature [42].

As expected, the results from ¹H NMR analysis indicated that in homoarm star products, the composition of ACMO and BA units was close to the initial monomer proportion, and in miktoarm star products, the arm composition ratio of l-PACMO to l-PBA (i.e., n_1/n_2) matched the designed feeding ratio of the two arm species. All final products had M_w , _{LS} over 100 kg/mol, with considerable star yields (over 70%) and arm numbers (around 35). Meanwhile, the intermediate purification process was avoided before the star formation step. Therefore, this continuous-flow synthesis strategy is highly attractive since it can directly convert reactants to star polymers with varied compositions for potential applications.

3.4. Star polymer products function as emulsifiers

Star polymer products with different arm and core structures would exhibit diverse properties. Typically, as the proportion of the PBA arms increased, the miktoarm star product SPA₂₅ precipitated out of the aqueous phase instead of being dissolved as SPA₇₅, which was attributed to the arm structure affected the hydrophobicity of the corresponding product. With a series of star products with tunable arm compositions in hand, we naturally investigated their potential application as emulsifiers in the toluene/water system. The residual linear chains in the star products were hard to be completely removed by precipitation, dialysis or other means, and thus such an arm separation procedure was omitted. Considering that the l-PBA arms were very hydrophobic, and the solubility of the hydrophilic l-PACMO in toluene was rather low, it can be deduced that the emulsifying performance of the star products should be mainly governed by the architectures of the star components.

Due to the protection from the arms, the cross-linked cores were hardly accessible to the external environment. The core fraction was reported to have limited effects on the emulsifying performance [43], and other parameters like arm numbers and arm chain lengths for these star products were controlled at a comparable level, hence the arm composition became the most critical variable to affect emulsifying abilities. As shown in Fig. 7, both miktoarm star and SPA products displayed the emulsifying ability to a certain degree, similar to sodium dodecyl sulfate (SDS, a common small-molecule emulsifier). For SPA, its hydrophilic PACMO arms and hydrophobic PHDDA cores help it to be efficiently anchored at the toluene/water interface, and can provide stability against the oil droplet coalescence, in a manner similar to the solid particles in Pickering emulsions [44]. For the miktoarm star products, they can adopt favorable configurations based on the composition of the flexible hydrophilic and hydrophobic arms, as to achieve enhanced residence at the toluene/water interface. When the incorporation of l-PBA became sufficiently higher (e.g., from MSPA₇₅ to MSPA₅₀), the affinity of these star stabilizers to the oil phase increased while the affinity to the aqueous phase decreased. Therefore, the aqueous-organic two-phase system would reverse from the oil-in-water emulsion to the water-in-oil emulsion (Fig. 7). For the homoarm star products with random copolymer arms, such as SPA₅₀, the short hydrophilic/hydrophobic segments had insufficient cohesive forces to anchor them firmly into the domains where they penetrate, thereby

weakening the self-assembly ability to form micelles [45]. For SPB, it was entirely dissolved by the oil phase (toluene) and no stable emulsion was formed.

Furthermore, the volumetric fraction of toluene in the toluene/water emulsion systems was varied, while the star products as the stabilizers were maintained at a concentration of 1 mg/mL. The emulsion samples were macroscopically evaluated in terms of the volume percentage of oil, emulsion and water phase on the 1st (Supporting Information, Table S2) and 7th day (Table 3) after preparation, which showed that the volume percentage of the emulsion phase in each sample remained almost unchanged (deviation below 5%) after seven days. As the toluene volumetric fraction increased from 15% to 70%, the oil-in-water emulsion system with the gradually rising emulsion volume percentage was formed for the MSPA₇₅ and SPA emulsion samples. In particular, the phase inversion occurred when the toluene volume fraction exceeded 50% for the MSPA₅₀ and MSPA₂₅ emulsion samples. In such cases, the oil phase transformed from the dispersed phase to the continuous phase. Interestingly, for the SPA emulsion sample with the toluene volumetric fraction of 60% or 70%, there existed three distinguished phases (Fig. S5), and the middle phase was an oil-in-water emulsion verified by the drop dilution method. The hydrophilic predominant SPA polymer tended to transfer into the water phase to form the oil-in-water type, even though it was initially dissolved in toluene [46]. A similar phenomenon also existed for the MSPA₂₅ emulsion sample with the toluene volumetric fraction of 15% or 30%.

The interfacial tension of the toluene/water two-phase system was lowered in the presence of SPA or miktoarm star products (see Table 4). The interfacial tension between pure toluene/water was 25.96 mN/m, according well with the literature value [47]. The adsorption of star products at the toluene/water interface can reduce the interfacial tension at a similar level to that of commercial emulsifier SDS. Among them, MSPA₅₀ was the most efficient to decrease the interfacial tension value to 1.36 mN/m, indicating that there could be an optimal balance between the hydrophilic and hydrophobic components of star polymers to realize the lowest interfacial tension. The emulsifying behavior could be affected by the stabilizer concentration [43], so we compared the critical micelle concentration (CMC) of the star product SPA with SDS (both in favor of forming oil-in-water type emulsion). As seen in Fig. 8, the CMC of the SPA was about 0.005 mg/mL, which was significantly lower than that of SDS (about 1 mg/mL). The much lower CMC value indicated that the stability of micelles formed from SPA was higher than that from SDS [48]. And we found that 1 mg/mL dosage of these star products could all stabilize emulsion systems for at least one month. Hence, star products directly obtained from the continuous operation should meet the requirements of being used as emulsifiers in various heterogeneous systems.

4. Conclusions

In this work, through combining the RAFT arm-first approach and microreactor technology, we succeeded in preparing star polymers with varied chain compositions in homemade cascade microreactor systems. First, the polymerization kinetics in the arm formation and star formation steps were studied. Then, we analyzed the effects (reaction time, mixing performance, and reactant formula) on the star yield and MWDs of the polymer products in detail. Moreover, through adjusting the flow ratio of streams for the arm and star formation steps, various arms could be prepared in parallel simultaneously, and a series of star products were prepared with varied compositions and amphiphilic properties. Finally, these star products were directly used as emulsifiers to stabilize the toluene/water system, since they could remarkably lower the interfacial tension. In all, this continuous-flow processing with the use of micro-reactors offers a facile example of converting commercial monomers to functional polymers under mild conditions, avoiding the intermediate purification, and can integrate the parallel synthesis of various chain components. In future work, polymers with specified structures

possessing stimuli-responsive and controllable self-assembly capabilities will be prepared in this developed continuous-flow platform.

Declaration of competing interest

The authors declare that they have no known competing financial interests or personal relationships that could have appeared to influence the work reported in this paper.

Acknowledgement

We would like to acknowledge financial support from the National Natural Science Foundation of China (No. 21676164) and the Science and Technology Commission of Shanghai Municipality (No. 18520743500) and the Shanghai Jiao Tong University Scientific and Technological Innovation Funds (No: 2019QYB06).

Appendix A. Supplementary data

Supplementary data to this article can be found online at <https://doi.org/10.1016/j.polymer.2021.123669>.

References

- [1] J.M. Ren, T.G. McKenzie, Q. Fu, E.H. Wong, J. Xu, Z. An, S. Shanmugam, T. P. Davis, C. Boyer, G.G. Qiao, Star polymers, *Chem. Rev.* 116 (2016) 6743–6836.
- [2] A. Blencowe, J.F. Tan, T.K. Goh, G.G. Qiao, Core cross-linked star polymers via controlled radical polymerisation, *Polymer* 50 (2009) 5–32.
- [3] S. Peleshanko, J. Jeong, R. Gunawidjaja, V. Tsukruk, Amphiphilic heteroarm PEO-b-PS m star polymers at the Air-Water interface: aggregation and surface morphology, *Macromolecules* 37 (2004) 6511–6522.
- [4] T.P. Lodge, A. Rasdal, Z. Li, M.A. Hillmyer, Simultaneous, segregated storage of two agents in a multicompartiment micelle, *J. Am. Chem. Soc.* 127 (2005) 17608–17609.
- [5] Z. Li, E. Kesselman, Y. Talmon, M.A. Hillmyer, T.P. Lodge, Multicompartiment micelles from ABC miktoarm stars in water, *Science* 306 (2004) 98–101.
- [6] Y. Gao, D. Zhou, J. Lyu, A. Sigen, Q. Xu, B. Newland, K. Matyjaszewski, H. Tai, W. Wang, Complex polymer architectures through free-radical polymerization of multivinyl monomers, *Nat. Rev. Chem.* 4 (2020) 194–212.
- [7] S. Kanaoka, M. Sawamoto, T. Higashimura, Star-shaped polymers by living cationic polymerization. 1. Synthesis of star-shaped polymers of alkyl and vinyl ethers, *Macromolecules* 24 (1991) 2309–2313.
- [8] J.G. Zilliox, P. Rempp, J. Parrod, Préparation de Macromolecules à Structure en Etoile, par Copolymerisation Anionique, *J. Polym. Sci., Part C: Polym. Sym.* 22 (1968) 145–156.
- [9] G.C. Bazan, R.R. Schrock, Synthesis of star block copolymers by controlled ring-opening metathesis polymerization, *Macromolecules* 24 (1991) 817–823.
- [10] S. Allison-Logan, F. Karimi, Y. Sun, T.G. McKenzie, M.D. Nothling, G. Bryant, G. G. Qiao, Highly living stars via core-first photo-RAFT polymerization: exploitation for ultra-high molecular weight star synthesis, *ACS Macro Lett.* 8 (2019) 1291–1295.
- [11] H. Gao, K. Matyjaszewski, Synthesis of star polymers by a new “core-first” method: sequential polymerization of cross-linker and monomer, *Macromolecules* 41 (2008) 1118–1125.
- [12] T.G. McKenzie, E.H. Wong, Q. Fu, A. Sulistio, D.E. Dunstan, G.G. Qiao, Controlled formation of star polymer nanoparticles via visible light photopolymerization, *ACS Macro Lett.* 4 (2015) 1012–1016.
- [13] J. Ferreira, J. Syrett, M. Whittaker, D. Haddleton, T.P. Davis, C. Boyer, Optimizing the generation of narrow polydispersity ‘arm-first’ star polymers made using RAFT polymerization, *Polym. Chem.* 2 (2011) 1671–1677.
- [14] H. Gao, K.J.M. Matyjaszewski, Synthesis of star polymers by a combination of ATRP and the “click” coupling method, *Macromolecules* 39 (2006) 4960–4965.
- [15] M. Qiu, L. Zha, Y. Song, L. Xiang, Y. Su, Numbering-up of capillary microreactors for homogeneous processes and its application in free radical polymerization, *React. Chem. Eng.* 4 (2019) 351–361.
- [16] Y. Su, K. Kuijpers, V. Hessel, T. Noël, A convenient numbering-up strategy for the scale-up of gas-liquid photoredox catalysis in flow, *React. Chem. Eng.* 1 (2016) 73–81.
- [17] C. Tonhauser, A. Natalello, H. Löwe, H. Frey, *Macromolecules* 45 (2012) 9551–9570.
- [18] N. Zaquet, M. Rubens, N. Corrigan, J. Xu, P.B. Zetterlund, C. Boyer, T. Junkers, Polymer synthesis in continuous flow reactors, *Prog. Polym. Sci.* 107 (2020) 101256.
- [19] N. Corrigan, R. Manahan, Z.T. Lew, J. Yeow, J.T. Xu, C. Boyer, Copolymers with controlled molecular weight distributions and compositional gradients through flow polymerization, *Macromolecules* 51 (2018) 4553–4563.
- [20] E. Baeten, J.J. Haven, T. Junkers, RAFT multiblock reactor telescoping: from monomers to tetrablock copolymers in a continuous multistage reactor cascade, *Polym. Chem.* 8 (2017) 3815–3824.
- [21] F.A. Leibfarth, J.A. Johnson, T.F. Jamison, Scalable synthesis of sequence-defined, unimolecular macromolecules by Flow-IEG, *Proc. Natl. Acad. Sci.* 112 (2015) 10617–10622.
- [22] Y. Su, Y. Song, L. Xiang, Continuous-flow microreactors for polymer synthesis: engineering principles and applications, *Top. Curr. Chem.* 376 (2018) 44.
- [23] S.T. Knox, N.J. Warren, Enabling technologies in polymer synthesis: accessing a new design space for advanced polymer materials, *React. Chem. Eng.* 5 (2020) 405–423.
- [24] L. Xiang, Y. Song, M. Qiu, Y. Su, Synthesis of branched poly (butyl acrylate) using the strathclyde method in continuous-flow microreactors, *Ind. Eng. Chem. Res.* 58 (2019) 21312–21322.
- [25] O. Eckardt, B. Wenn, P. Biehl, T. Junkers, F.H. Schacher, Facile photo-flow synthesis of branched poly(butyl acrylate)s, *React. Chem. Eng.* 2 (2017) 479–486.
- [26] P. Sun, J.A. Liu, Z.B. Zhang, K. Zhang, Scalable preparation of cyclic polymers by the ring-closure method assisted by the continuous-flow technique, *Polym. Chem.* 7 (2016) 2239–2244.
- [27] B. Wenn, A. Martens, Y.-M. Chuang, J. Gruber, T. Junkers, Efficient multiblock star polymer synthesis from photo-induced copper-mediated polymerization with up to 21 arms, *Polym. Chem.* 7 (2016) 2720–2727.
- [28] P. Ye, P.F. Cao, Q. Chen, R. Advincula, Continuous flow fabrication of block copolymer-grafted silica micro-particles in environmentally friendly water/ethanol media, *Macromol. Mater. Eng.* 304 (2019) 1800451.
- [29] D. Wang, W.J. Wang, B.G. Li, S. Zhu, Semibatch RAFT polymerization for branched polyacrylamide production: effect of divinyl monomer feeding policies, *AIChE J.* 59 (2013) 1322–1333.
- [30] J.H. Vrijen, C.O. Medeiros, J. Gruber, T. Junkers, Continuous flow synthesis of core cross-linked star polymers via photo-induced copper mediated polymerization, *Polym. Chem.* 10 (2019) 1591–1598.
- [31] M.J. Monteiro, J. de Barbeyrac, Free-radical polymerization of styrene in emulsion using a reversible addition–fragmentation chain transfer agent with a low transfer constant: effect on rate, particle size, and molecular weight, *Macromolecules* 34 (2001) 4416–4423.
- [32] P. Ye, P.F. Cao, Z. Su, R. Advincula, Highly efficient reversible addition–fragmentation chain-transfer polymerization in ethanol/water via flow chemistry, *Polym. Int.* 66 (2017) 1252–1258.
- [33] L. Xiang, W.J. Wang, B.G. Li, S. Zhu, Tailoring polymer molecular weight distribution and multimodality in RAFT polymerization using tube reactor with recycle, *Macromol. React. Eng.* 11 (2017) 1700023.
- [34] C.H. Hornung, X. Nguyen, S. Kyi, J. Chieffari, S. Saubern, Synthesis of RAFT block copolymers in a multi-stage continuous flow process inside a tubular reactor, *Aust. J. Chem.* 66 (2013) 192–198.
- [35] W.-J. Wang, D. Wang, B.-G. Li, S. Zhu, Synthesis and characterization of hyperbranched polyacrylamide using semibatch reversible addition–fragmentation chain transfer (RAFT) polymerization, *Macromolecules* 43 (2010) 4062–4069.
- [36] F. Zhong, Y. Zhou, M. Chen, The influence of mixing on chain extension by photo-controlled/living radical polymerization under continuous-flow conditions, *Polym. Chem.* 10 (2019) 4879–4886.
- [37] Y. Song, M. Shang, G. Li, Z.-H. Luo, Y. Su, Influence of mixing performance on polymerization of acrylamide in capillary microreactors, *AIChE J.* 64 (2018) 1828–1840.
- [38] M.H. Reis, T.P. Varner, F.A. Leibfarth, The influence of residence time distribution on continuous-flow polymerization, *Macromolecules* 52 (2019) 3551–3557.
- [39] H. Gao, K. Matyjaszewski, Structural control in ATRP synthesis of star polymers using the arm-first method, *Macromolecules* 39 (2006) 3154–3160.
- [40] J. Peng, C. Tian, L. Zhang, Z. Cheng, X. Zhu, The in situ formation of nanoparticles via RAFT polymerization-induced self-assembly in a continuous tubular reactor, *Polym. Chem.* 8 (2017) 1495–1506.
- [41] P. Liu, E. Landry, Z. Ye, H. Joly, W.-J. Wang, B.-G.J.M. Li, “Arm-first” synthesis of core-cross-linked multiarm star polyethylenes by coupling palladium-catalyzed ethylene “living” polymerization with atom-transfer radical polymerization, *Macromolecules* 44 (2011) 4125–4139.
- [42] A. Takano, M. Okada, T.J.P. Nose, Arm-number dependence of dimensions of star-shaped polystyrene in a good solvent, *Polymer* 33 (1992) 783–788.
- [43] W. Li, Y. Yu, M. Lamson, M.S. Silverstein, R.D. Tilton, K. Matyjaszewski, PEO-based star copolymers as stabilizers for water-in-oil or oil-in-water emulsions, *Macromolecules* 45 (2012) 9419–9426.
- [44] B.P. Binks, S.O. Lumsdon, Influence of particle wettability on the type and stability of surfactant-free emulsions, *Langmuir* 16 (2000) 8622–8631.
- [45] M. Matos, B. Favis, P. Lomellini, Interfacial modification of polymer blends—the emulsification curve: 1. Influence of molecular weight and chemical composition of the interfacial modifier, *Polymer* 36 (1995) 3899–3907.
- [46] X. Shi, M. Miao, Z. An, Core cross-linked star (CCS) polymers with tunable polarity: synthesis by RAFT dispersion polymerization, self-assembly and emulsification, *Polym. Chem.* 4 (2013) 1950–1959.
- [47] A. Bak, W. Podgorska, Interfacial and surface tensions of toluene/water and air/water systems with nonionic surfactants Tween 20 and Tween 80, *Colloid. Surface.* 504 (2016) 414–425.
- [48] Y. Nagasaki, T. Okada, C. Scholz, M. Iijima, M. Kato, K.J.M. Kataoka, The reactive polymeric micelle based on an aldehyde-ended poly (ethylene glycol)/poly (lactide) block copolymer, *Macromolecules* 31 (1998) 1473–1479.